Structure Monitoring using Wireless Sensor Networks

CS294-1 Deeply Embedded Network Systems

Sukun Kim
Department of Electrical Engineering and Computer Sciences
University of California, Berkeley

Abstract

Structure monitoring brings new challenges to wireless sensor network: high-fidelity sampling, collecting large volume of data, and sophisticated signal processing. New accelerometer board measures tens of µG acceleration. High frequency sampling is enabled by new component of David Gay. With new component, up to 6.67KHz sampling is possible with jitter less than 10µs. Large-scale Reliable Transfer (LRX) component collects data at the expense of 15% penalty of channel utilization for no data loss. To overcome low signal-to-noise ratio, analog low-pass filter is used, and multiple digital data are averaged. Structure monitoring is a driving force for extending capability of wireless sensor networks system.

1. Introduction

Wireless sensor network enables low-cost sensing of environment. Many applications using wireless sensor networks have low duty cycle and low power consumption. However the ability of wireless sensor networks can be extended in reverse way. Enhanced TinyOS, and new components opened possibility for more aggressive applications. Structure monitoring is one example of such applications.

To monitor a structure (e.g. bridge, building), we measure behavior (e.g. vibration, displacement) of structure, and analyze health of the structure based on measured data. Figure 1 shows overall system. Each component can have multiple subcomponents. In our case, sensor is accelerometer which will be discussed in Section 2, and analog processing has low-pass filter (Section 6.) Digital processing includes averaging (Section 6), data collection (Section 5), and system identification (Section 6). Low-jitter control contains high-frequency sampling (Section 4). There are more sub-components to be added in the future: time synchronization in low-jitter control, calibration and digital filtering in digital processing.

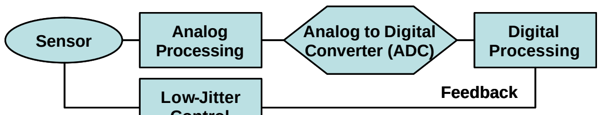

Figure 1 Overall System

Here we present challenges, findings, and our experience in structure monitoring using wireless sensor networks. Rather than focusing on one single component, this paper overview overall system and issues in each component.

2. Related Work

Habitat monitoring is a leading application of wireless sensor network. And it is an example application with low duty cycle. ZebraNet [1] uses PDA-level device with 802.11b wireless network. Great Duck Island [2] uses Berkeley mote, and watch ducks without disturbing them at low cost.

For structure monitoring, there are tremendous amount of research using conventional wired way. GPS was used combined with wired data collection [3, 4], however at a high cost. There is an approach using wireless network for data collection [5], which has great advantage over wired network. However, it uses large hardware platform (in terms of size, power, and cost) which diminishes benefit of wireless approach. [6] uses low-cost device and wireless network, but it is more like conceptual test, and fidelity is not sufficient for real deployment. We begins with high fidelity sampling in the following section.

3. Data Acquisition

Data acquisition is composed of mainly two parts: data sampling, and data collection. Structure monitoring requires high fidelity data sampling. Accurate, high frequency sampling, and low jitter are main requirement for high quality sample. Accuracy is discussed in this section, and high frequency sampling with low jitter will be covered in Section 4. And data collection will be discussed in Section 5.

In structure monitoring, acceleration signal is very week. Detecting even moderate earthquake requires to measure 500μG acceleration. Sensitivity and accuracy of accelerometer is crucial, so we put significant portion of effort to accelerometer board. New accelerometer board was designed by as shown in Figure 2.

3.1. Accelerometers

It has two kinds of accelerometers: ADXL 202E, Silicon Designs 1221L. Table 1 shows characteristics of each accelerometer combined with entire system. Accelerometer board contains 1 of ADXL 202E, and 2 of Silicon Designs 1221L, and 4 16bit analog to digital converter (ADC). There are two channels for ADXL 202E, and two channels for Silicon Designs 1221L with same orientation. One is parallel to gravity, and the other is vertical to gravity. Initially both accelerometers had range of -2G ~ 2G, but for better sensitivity, range of Silicon Designs 1221L is change to -0.1G ~ 0.1G. Channel with axis parallel to gravity has 1G offset to compensate for offset by gravity. It also contains one temperature sensor (reason will be explained later). New version of Berkeley mote, named as Mica2 [7], is used for control and communication.

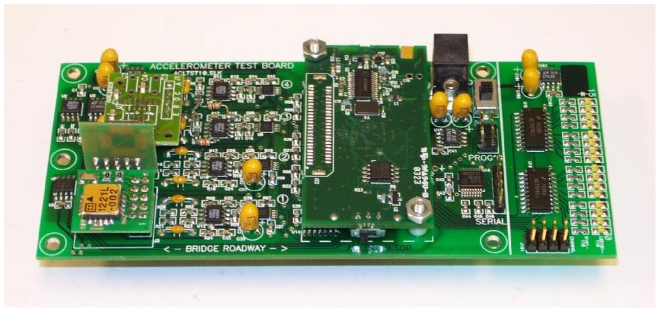

Figure 2 Accelerometer Board

Table 1 Two Accelerometers Combined with System

	ADXL 202E	Silicon Designs 1221L
Type	MEMS	MEMS
Number of axis	2	1
Range	-2G ~ 2G	-0.1G ~ 0.1G
System noise floor	200(μG / vHz)	30(μG / vHz)
Price	$10	$150

3.2. Noise Floor Test and Shaking Table Test

To see static characteristic of accelerometers, accelerometer board was put to quiet place (from vibration and sound) with constant temperature. This test shows noise floor which is shown in Table 1. For Silicon Designs 1221L, range was -0.1G ~ 0.3G. Then to see dynamic behavior of accelerometers, we performed shaking table test with constant temperature. Even though test site was not completely free from vibration and sound noise, it was quiet enough for a dynamic range of shaking table to dominate noise. Results are shown in Figure 3. Left figure is result of ADXL 202E, right one is result of Silicon Designs 1221L, and driving frequency is 0.5Hz. Data are read from both channels at the same time. For this test, channel for Silicon Designs 1221L had range of -2G ~ 2G.

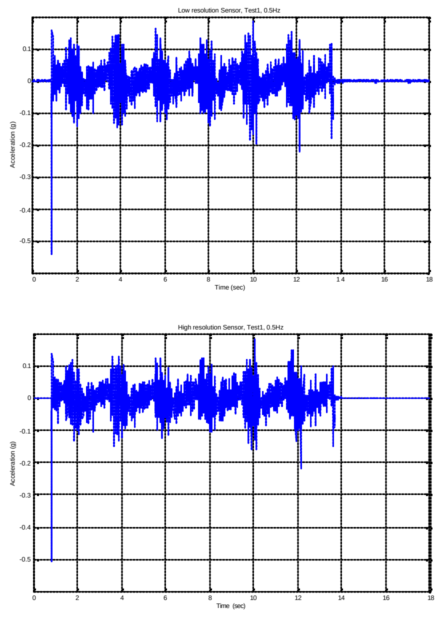

Figure 3 Shake Table Test (0.5Hz)

We can see Silicon Designs 1221L shows cleaner shape in both static situation and dynamic situation. Figure 4 show another experiment on shaking table. Here frequency increases while displacement remains constant. When movement gets rigorous, Silicon Designs 1221L does not properly read it. It seems like Silicon Designs 1221L has larger damping factor than ADXL 202E.

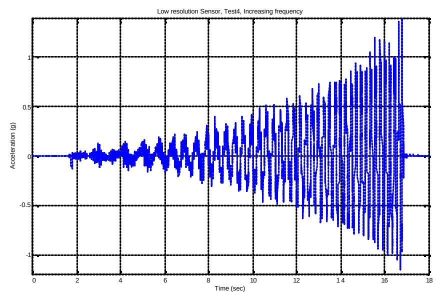

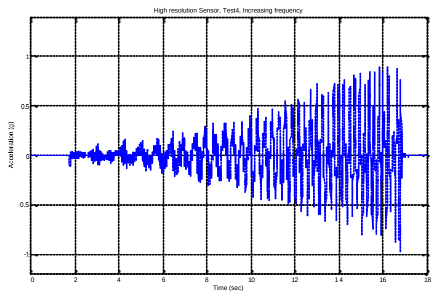

Figure 4 Shaking Table Test (Increasing frequency with same displacement)

3.3. Tilting Test and Vault Test

To measure linearity of accelerometer value, we performed tilting test with help of Bob Uhrhammer. By changing tilting degree of accelerometer, we can obtain line showing acceleration value read versus real acceleration. Only channel vertical to gravity is measured of Silicon Designs 1221L. For this test, range was -0.1G ~ 0.3G. Deviation from minimum mean square error line is within 60μG

For a better noise floor test, we went to a vault in Lawrence Berkeley Laboratory. Figure 5 shows how quiet inside of vault is compared to normal office environment. And it also shows reference reading from very sophisticated accelerometer in the vault, which is used for seismic research. System with Silicon Designs 1221L shows 20dB higher noise level. Figure 6 shows time plot of acceleration in vault and office environment for 30 minute period. Red line shows noise in normal office environment. We can see noise from machines, which is also visible in Figure 5. Blue line shows acceleration readings from vault. Drift is observed in this case. On test day, it was cold, and inside of vault was hot by lights. We put accelerometer in a vault, and immediately started sampling. So accelerometer board was under drastic change in temperature. Drift is almost 10mG which is significant compared to noise floor, and sensitivity. More discussion on temperature will follow in Section 8 Future work.

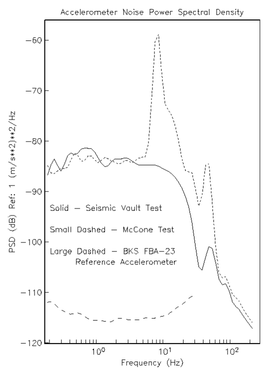

Figure 5 Noise Power Spectral Density

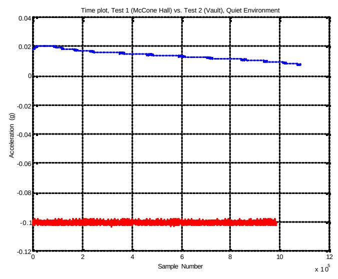

Figure 6 Time Plot of Acceleration

4. High-frequency Sampling

Characteristic vibration frequency of a structure is usually around 10Hz rage. However by Nyquist theorem, sampling rate should be at least twice of that. Moreover, to reduce effect of noise averaging is used, and sampling rate is multiplied by the number of samples averaged. All these factors increase sampling rate to KHz level. Structure monitoring requires regular sampling with uniform interval, and jitter becomes harder problem as sampling rate gets higher. There are two kinds of sources to jitter, and they are shown in Figure 7. Temporal jitter occurs inside of node, because actual sampling does not occur at uniform interval. So even with only one node, temporal jitter happens. Spatial jitter happens because of variation in hardware, and imperfect time synchronization. Even if two nodes agree to sample at time T, this T occurs at different absolute times for those two nodes. Spatial jitter occurs only when there are more than one node. Here only temporal jitter is considered. Spatial jitter will be discussed in Section 8 Future Work.

David Gay wrote a new component HighFrequencySampling, which enables KHz range sampling. This new component is introduced in Section 4.1, jitter test result is shown in Section 4.2, and theoretical jitter analysis follows in Section 4.3.

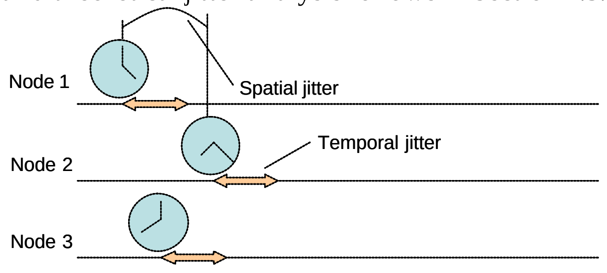

Figure 7 Sources of Jitter

4.1. HighFrequencySampling component

This component is written by David Gay for sampling at KHz level frequency. Pre-existing components can sample only up to 200Hz. There are two major sub-components which enable high frequency sampling.

MicroTimer is a new timer component which directly accesses hardware timer, and does not provide multiple abstract timers. This is very simple and quick to process timer events. BufferLog is a flash memory writer. It has two buffers. One is filled up by upper layer application while the other buffer is written to flash memory as a background task. Those two components (MicroTimer, BufferLog) have minimum amount and length of atomic section, which blocks other operation and could introduce queue overflow.

With HighFrequencySampling component, 6.67KHz sampling is achieved. With averaging 16 samples, 1KHz is achieved, which means 16KHz of sampling.

4.2. Jitter Test

We tested jitter of HighFrequencySampling component. Instead of storing acceleration value, time is recorded so that we can measure jitter. Figure 8 shows jitter as time goes. There are two sections: plain section, spiky section, even though at 6.67KHz this separation is not clear. These two sections constitute one epoch. It takes epoch period of time to fill up buffer. During spiky period, buffer is written to flash memory as a background task. At 1KHz, only small portion of sampling is affected by flash memory write. At 6.67KHz, flash memory write takes too much portion of time to fill up buffer, most of sampling are affected by flash memory write. Looking at 5KHz case, even at 6.67KHz flash memory write should not affect that many sampling. However, overhead of sampling itself seems to have some effect.

There is another thing interesting. At plain section, there is a constant delay for every sampling. This delay is wake up time of CPU. When CPU is idle, it enters a sleeping mode. And it takes 4 cycles to recover. Since there is a function call to record time, actually it takes 5 cycles here. Since CPU runs at 8MHz, this wakeup time is equal to 625ns.

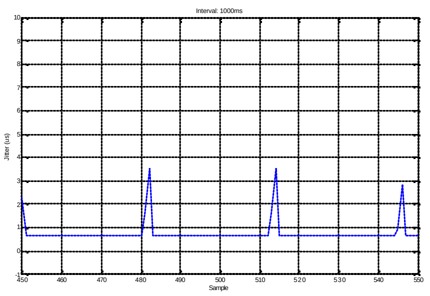

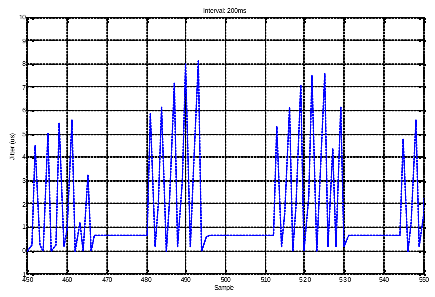

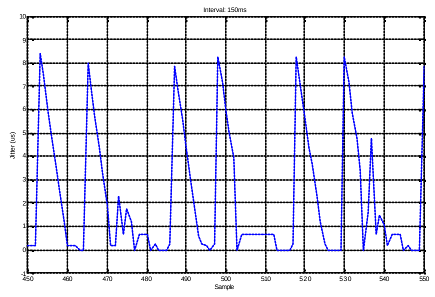

Figure 8 Jitter in Time Line (1KHz, 5KHz, 6.67KHz respectively)

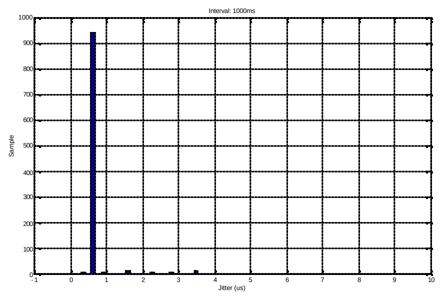

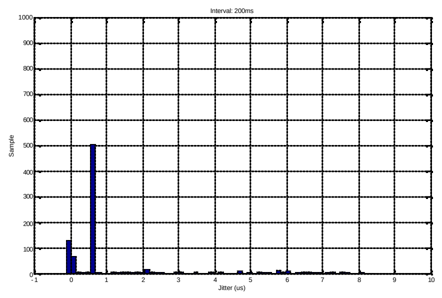

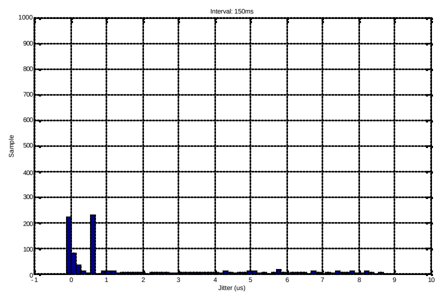

Figure 9 Histogram of Jitter (1KHz, 5KHz, 6.67KHz respectively)

Figure 9 shows distribution of jitter values (histogram). We can see a peak at 625ns, which is wakeup time. Except this peak, frequency of jitter is largest near 0μs, and gradually decreases as jitter value increases. And jitter values are within 10μs. Next section analyzes this phenomenon.

4.3. Jitter Analysis

Figure 10 shows interaction of sampling and other job (flash memory write). Timer event for sampling occurs regularly with uniform interval. However to be serviced in CPU, CPU should finish non-preemptible portion (in TinyOS, atomic section). Then CPU handles events in event queue which came before timer event. Then finally timer event for sampling is handled. For our case, event queue is not likely filled with other waiting events, so this possibility is not considered here. Then the length of atomic section in execution determines jitter.

Let T(i) be execution time of atomic section i, and let X(i) be a random variable uniformly distributed in [0, T(i)]. And let C be context switch time. Assume that the probability of timer event occurring at any point in atomic section i is same, then jitter will follow C+X(i). Figure 11 shows this jitter model, where F(i) is frequency of occurrence of atomic section i.

Since jitter distribution of every atomic section begins from C, the frequency is highest near C and decreases as moving farther. And frequency drop at C+T(i) by F(i), since atomic section i will not have any distribution beyond C+T(i).

Actually there is a peak at C, because when program is in preemptible section, it will immediately service timer event after context switch time C.

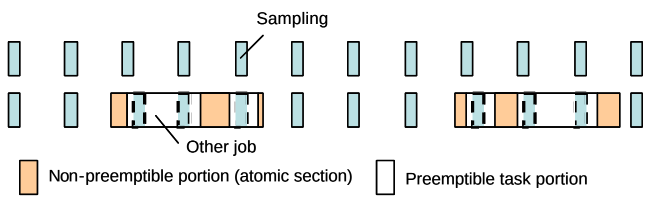

Figure 10 Occurrence of Jitter

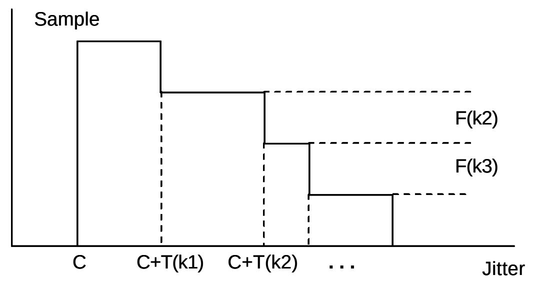

Figure 11 Jitter Model

Test result matches quite well with theoretical model here. And we can also notice that context switch time C is 0, which means timer event is handled immediately if program is not in atomic section. There is one bad news. Worst case jitter is determined by the longest atomic section of the entire system. So even if we have good component at low layer, if upper application layer is not well written, system will suffer long worst case jitter.

High frequency sampling with high accuracy produces a large amount of data. This large amount of data can not be collected at real time through wireless communication. So we store data to flash first. And after sampling enough data, collection starts, and data in flash memory are transferred. Transferring large amount of data is another challenge. Next Section explains how we transfer huge volume of data efficiently.

5. Large-scale Reliable Data Transfer

As we sample at high frequency with large number of nodes, the amount of data gets large quickly. Let us assume each node store 4Byte of data and 4Byte of time stamp at 100Hz. And assume there are 100 nodes, radio throughput is 1.2KB/s, and data is collected to one base station. If acceleration data worthy 5 minutes is collected, each node will transfer 240,000Bytes. 100 nodes will transfer 24,000,000Bytes. Since the end link to base station is a bottleneck, it will take more than 5 hours. We can see bandwidth is narrow compared to aggressive data sampling. Even if we alleviate this problem using multi-channel or multi-tier network, still we will be in short of bandwidth.

Moreover, we need to transfer data reliably. We will be able to overcome some packet losses using data processing, but at current stage we do not assume this technique.

These needs lead to efficient large-scale reliable data transfer. Right now RAM to RAM transfer is implemented as a building block. Multi-hop flash memory to flash memory transfer will be discussed in Section 8 Future Work.

5.1. Protocol

Large-scale Reliable Transfer (LRX) component assumes that data resides in RAM. Upper layer should handle non-volatile storage. LRX transfers one data cluster, which is composed of several blocks. One block fits into one packet, so the number of blocks is equal to window size. Each data cluster has a data description. After looking at data description, receiver may deny data (receiver already has that data, or that data is not useful anymore).

Explicit open handshake is used. Data description and size of cluster is sent as a transfer request. If receiver has enough RAM, and application layer agrees on data description, then receiver sends acknowledgement for transfer request.

Once connection is established, actual data is transferred. Protocol at high level can be summarized as selective acknowledgement and retransmission. Data transfer is composed of multiple rounds. In each round, sender sends packets missing in the previous round. At the end of each round, receiver sends acknowledgement saying which packets are missing. Then sender, after looking at this acknowledgement, sends packet missing again. The first round can be thought of as a special case where every packet was missing in the previous (imaginary) round.

Tear-down is implicit. Successful tear-down cannot be guaranteed anyway, however close phase will introduce overhead, and delay. We favored quick movement to next connection, and eliminated close phase.

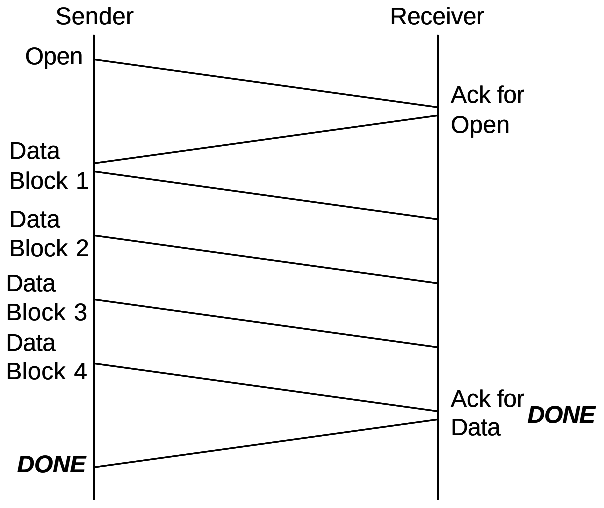

Figure 12 No Lost Packet

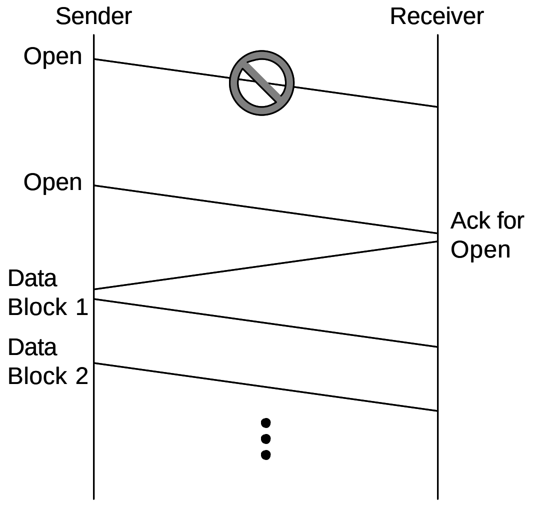

Figure 13 Open is lost

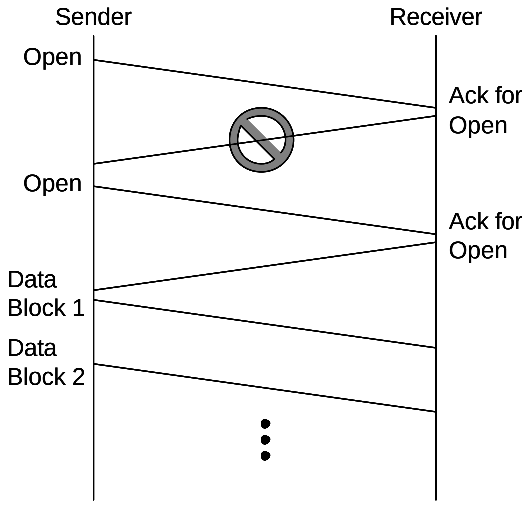

Figure 14 Ack for Open is lost

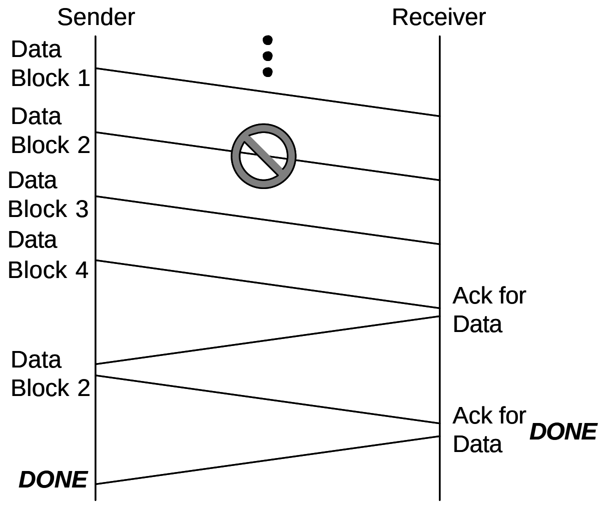

Figure 15 Data Block 2 is lost

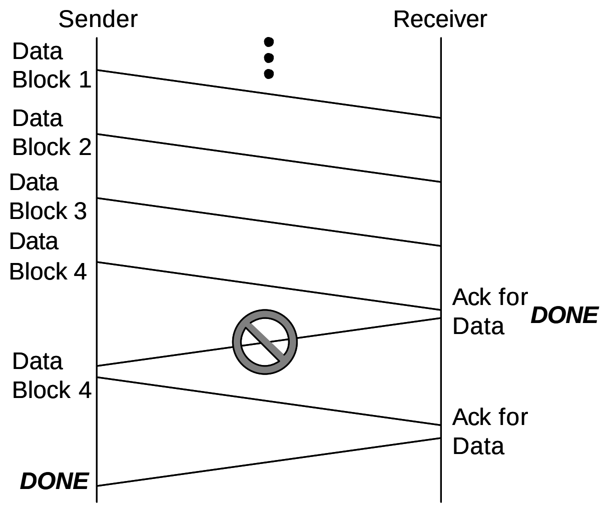

Figure 16 Ack for Data is lost

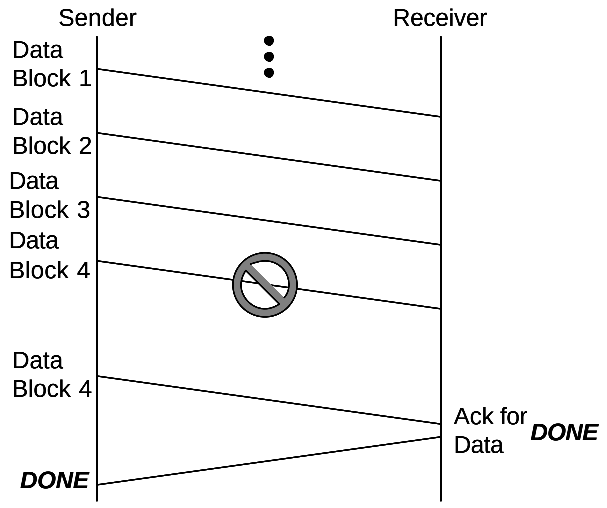

Figure 17 Data Block 4 is lost (no timeout to send ack)

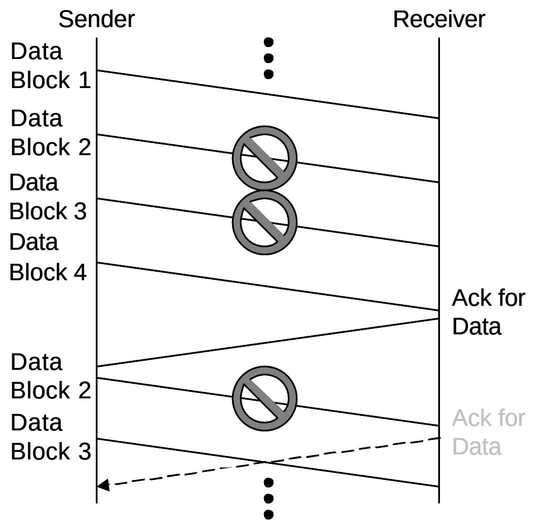

Figure 18 After Ack, when the first Data is lost

Any packet can be lost during transfer, so there is timeout for every wait to prevent indefinite waiting.

Figure 12 shows case with no packet loss. When Open packet is lost as in Figure 13, Open is retransmitted after timeout. When Ack for Open is lost as in Figure 13Figure 14, Open is retransmitted also after timeout. Figure 15 shows what happens if Data packet is lost. After looking at acknowledgement, sender resends lost data. Figure 16 shows when Ack for data is lost. Sender times out. This is clearer in Figure 17. As shown, receiver does not timeout to send Ack.

There are two reasons why only sender times out and stimulate receiver for Ack. The first reason is shown in Figure 16. If sender doesn't time out, for a receiver to make sure Ack is delivered to sender, receiver should get acknowledgement from sender for Ack itself. This is not good. So it is clear that sender should timeout. Given that sender times out, timeout of receiver makes no difference except that channel is wasted by unnecessary Ack from receiver. So timeout in only sender side is desirable. As a second reason, if receiver times out, in case like Figure 18 (if first Data after Ack is lost), second Data always collide with resent Ack of receiver. This is not a good phenomenon. Therefore, after sending last packet in each round, if acknowledgement does not come, sender sends the last packet in that round again to stimulate acknowledgement. However, this does not mean receiver has no timeout. Receiver waits sufficient amount of time, and if nothing happens, it regards the situation as a failure.

Figure 19 shows state transition diagram of sender, and Figure 20 shows state transition diagram of receiver.

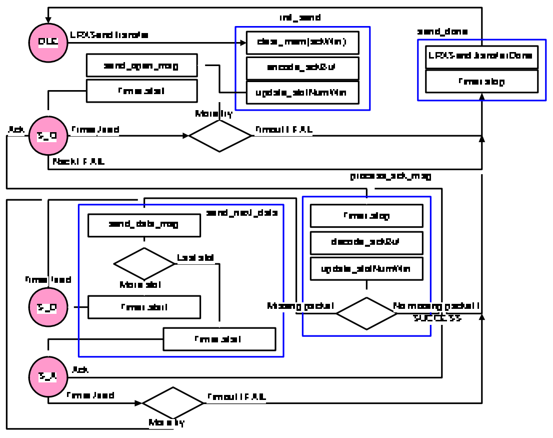

Figure 19 State Transition Diagram of Sender

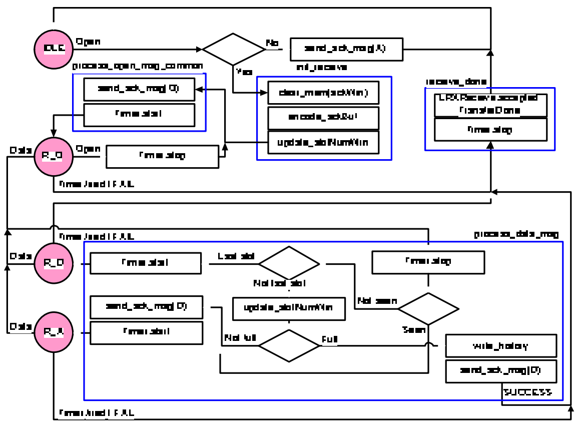

Figure 20 State Transition Diagram of Receiver

5.2. Evaluation

Two performance metrics are evaluated: throughput, robustness. Robustness is partially tested by looking at whether LRX successfully works under high loss rate.

There are three factors which determine throughput: interval between packets, window size, and loss rate.

Interval between packets is controlled by timer not to saturate channel. Now throttle is fixed at 10 packets per second. Better way would be throttling sending rate by looking at channel quality, like loss rate. This issue will be discussed more in Section 8 Future Work. For tests here, fixed rate (10 packets per second) is used.

Window size determines relative overhead of control packets (open session, acknowledgement). Therefore, as window size increases, throughput also increases. Figure 21 shows test result. Optimal case is when window size is infinite. For the case with window size 16, throughput is 88% of optimal case. Considering loss rate of 3%, actual relative throughput is 91%, which is higher than 85% of channel utilization ratio. This is because 1) LRX tag overhead is included for optimal case, 2) control packets do not follow 10 packets/s.

Loss rate determines overhead for retransmissions for lost packets. As loss rate increases, retransmission increases, and throughput decreases. Figure 22 shows the result. This graph also shows robustness of LRX. Even with loss rate above 20%, LRX successfully transfers data.

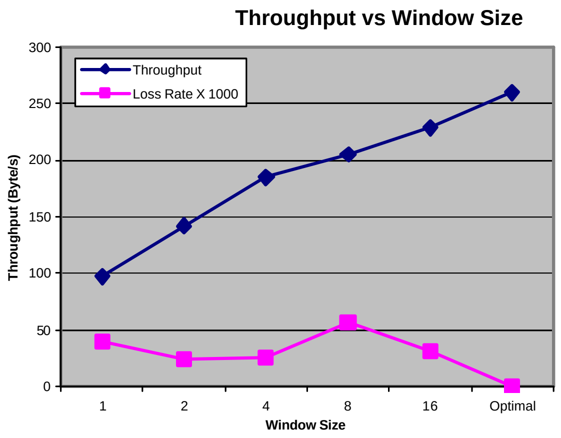

Figure 21 Throughput vs Window Size

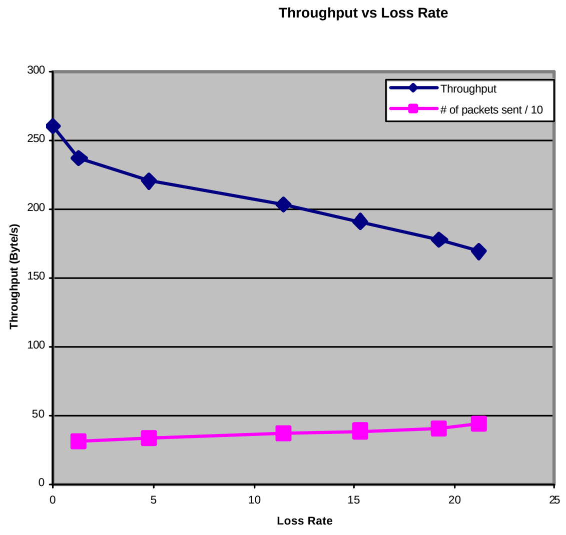

Figure 22 Throughput vs Loss Rate

Table 2 Channel Utilization

	TOS_Msg	LRX (only data)	LRX (Window Size 16)
Total Data (bytes)	36	36	613
Meta Data (bytes)	7	10	197
Real Data (bytes)	29	26	416
Channel Utilization (%)	78.38	72.22	67.86
Comparison to TOS_Msg (%)	100	89.66	84.24

Table 2 shows channel utilization for TOS_Msg, and data message of LRX, and overall LRX. TOS_Msg has an overhead of 7 bytes, and LRX data has 3 bytes overhead. Inclusion of overhead of control message further decreases channel utilization. LRX (data only) is the theoretical limit of LRX (when window size is infinite). We can see that using LRX lowers channel utilization by 15%.

6. Signal Processing and System Identification

As an analog signal processing low-pass filter is used, which filters high frequency noise. However as shown in Figure 23, loss-pass filter is not perfect, and there exists some leftover signal above threshold frequency. Therefore even if low-pass filter is used, sampling frequency at ADC should be higher than threshold frequency of low-pass filter. Moreover by Nyquist theorem, to avoid aliasing, sampling rate should be at least twice of signal's frequency. For accelerometer board, low-pass filter with threshold frequency 25Hz is used. Then ADC should sample at frequency much higher than 50Hz.

As a digital signal processing, averaging is used. If noise follows Gaussian distribution, by averaging N numbers, noise decreases by a factor of sqrt(N). This multiplies sampling frequency by a factor of N. Currently averaging is optionally used for testing.

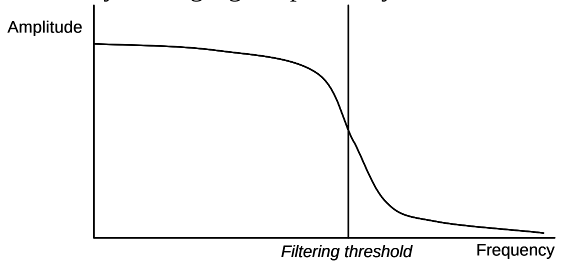

Figure 23 Imperfect Loss-pass Filter

System identification is identifying model of target system. By matching input to system and output from system, we can construct a mathematical system model. Usual process is fitting a general Box-Jenkins multi-input multi-output model to sampled data. And natural frequencies, damping ratios and mode shape are then estimated using the estimated Box-Jenkins model. Most part of system identification is to be done in the future.

7. Conclusion

New challenges are analyzed which are brought by structure monitoring to wireless sensor network. High accuracy accelerometer, high frequency sampling with low jitter, low-pass filter, averaging, large-scale reliable data collection, they all were not critical issues in conventional application of wireless sensor networks. Those challenges are overcome to sufficient degrees, however there are still many problems to be solved.

Figure 24 shows accelerometer accuracy and diverse challenges which will be encountered in pursuit of each degree of accuracy. It is straightforward that to achieve higher accuracy target, we should overcome more challenges. Those challenges in the figure are only a subset of already recognized problems. We can expect unrecognized problems will give additional challenges. However, as we can see in Figure 25, the extent of applications enabled also increases, as accuracy increases.

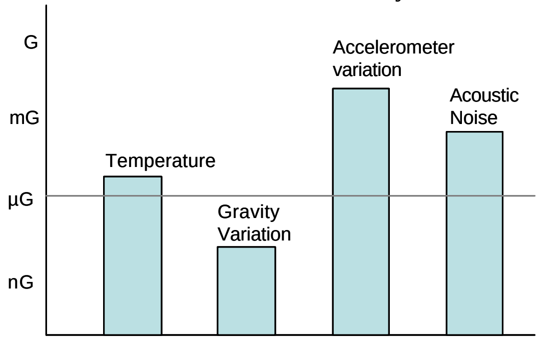

Figure 24 Challenges versus Accuracy

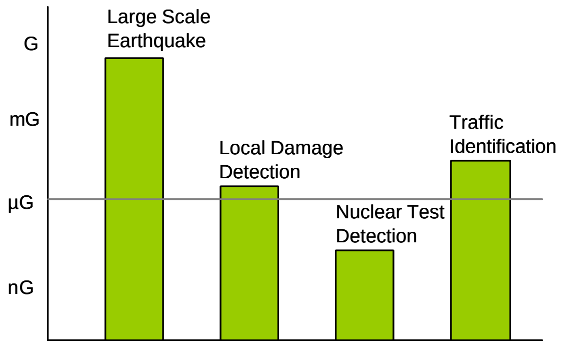

Figure 25 Possible Applications versus Accuracy

8. Future Work

Accelerometer should be calibrated with respect to temperature. Industry uses even 5th order polynomial for calibration. It requires a huge amount of effort. This is not feasible in our case. First, calibration cost is too high for low cost wireless sensor networks. Second, computation like 5th order polynomial for each sample is too expensive in lese powerful, low cost devices. Therefore de-trending at server side will be a good solution. After stamping each data or each set of data with temperature, we can process later.

Temporal jitter is handled by high frequency sampling component. Spatial jitter should be solved by time synchronization. ITP [8] is a time synchronization protocol widely used in Internet. In wireless sensor network, there were several studies.

In RBS [9], synchronization is done among receivers, eliminating sender's jitter in media access. TPSN [10] put time stamp after obtaining channel. This gives even better synchronization accuracy than RBS (10μs compared to 20μs). Still there is a source of jitter at receiver side. As we saw in jitter for sampling, handling interrupt by radio can be delayed by atomic section of other activity. As suggested in [10], putting time stamp at MAC layer in receiver side will eliminate this jitter.

To maximize utility of channel, we need to monitor channel quality (loss rate), and throttle packet injection rate accordingly. This is very like media access control, just at higher level. This requires eavesdropping channel, and needs access to lower network layer breaking hierarchy.

LRX transfers data from RAM to RAM. Using LRX as a building block, multi-hop data collection need be implemented. Exploiting linear geography of bridge, pipelining can be used. Multi-channel can distribute traffic over multiple frequency spectrum and increase throughput. Supernode like Stargate can be also used.

As a digital signal process, digital low-pass filter can be used, to eliminate effect of imperfect analog low-pass filter.

9. Acknowledgement

This work is a part of 'Structural Health Monitoring of the Golden Gate Bridge' project with David Culler, James Demmel, Gregory Fenves, Tom Oberheim, and Shamim Pakzad. This work is supported, in part, by the National Science Foundation under Grant No. EIA-0122599. Thank to Rabin Patra and Sergiu Nedevschi for extensive discussion over LRX protocol design. Robert Szewczyk gave critical comment and help to jitter analysis. And Philip Buonadonna gave important feedback for interface and protocol of LRX.

10. Reference

[1] Philo Juang, Hide Oki, Yong Wang, Margaret Martonosi, Li-Shiuan Peh, Daniel Rubenstein. Energy-Efficient Computing for Wildlife Tracking: Design Tradeoffs and Early Experiences with ZebraNet, in Proceedings of ASPLOS-X, San Jose, October 2002.
[2] Alan Mainwaring, Joseph Polastre, Robert Szewczyk, David Culler, John Anderson. Wireless Sensor Networks for Habitat Monitoring, in the 2002 ACM International Workshop on Wireless Sensor Networks and Applications. WSNA '02, Atlanta GA, September 28, 2002.
[3] Clement Ogaja, Chris Rizos, Jinling Wang, James Brownjohn. Toward the Implementation of On-line Structural Monitoring Using RTK-GPS and Analysis of Results Using the Wavelet Transform.
[4] Penggen Cheng, Wenzhong John Shi, Wanxing Zheng. Large Structure Health Dynamic Monitoring Using GPS Technology.
[5] Juan M. Caicedo, Johannio Marulanda, Peter Thomson, and Shirley J. Dyke. Monitoring of Bridges to Detect Changes in Structural Health, in the Proceedings of the 2001 American Control Conference, Arlington, Virginia, June 25–27, 2001.
[6] Jerome Peter Lynch, Anne S. Kiremidjian, Kincho H. Law, Thomas Kenny and Ed Carryer. Issues in Wireless Structural Damage Monitoring Technologies, in the Proceedings of the 3rd World Conference on Structural Control (WCSC), Como, Italy, April 7-12, 2002.
[7]
http://webs.cs.berkeley.edu/tos/hardware/hardware.html
[8] Mills, D.L. Internet time synchronization: the Network Time Protocol. IEEE Trans. Communications 39, 10 (October 1991), 1482-1493.
[9] Jeremy Elson, Lewis Girod and Deborah Estrin. Fine-Grained Network Time Synchronization using Reference Broadcasts, in Proceedings of the Fifth Symposium on Operating Systems Design and Implementation (OSDI 2002), Boston, MA. December 2002.
[10] Saurabh Ganeriwal, Ram Kumar, Mani B. Srivastava. Timing-Sync protocol for Sensor Networks, in SenSys '03, November 5-7, 2003, Los Angeles, California, USA.